Adsorption thermodynamics and kinetics of disperse dye on poly(*p*-phenylene benzobisoxazole) fiber pretreated with polyphosphoric acid

Yu Guan*,**, Ya-hong Mao***, Dong Wei**, Xiu-xing Wang****, and Pu-xin Zhu*,†

*Textile Institute, Sichuan University, Chengdu 610065, P. R. China
**Bureau of Quartermaster Military Representation of the General Logistics Department, PLA, Beijing 100071, P. R. China
***Department of Dyeing and Chemistry, Chengdu Textile College, Chengdu 611731, P. R. China
****Quartermaster Equipment Institute of General Logistics Department, PLA, Beijing 100010, P. R. China

Abstract−Adsorption thermodynamic and kinetic studies of C. I. disperse dye 60 on PBO fiber pretreated with polyphosphoric acid (PPA) were carried out under the conditions of pH 6.0±0.2, initial dye concentration 0.05-1.0 g/L and liquor ratio 2,000 : 1. The results showed that the equilibrium adsorption isotherm of the disperse dye on the pretreated PBO fiber was a Langmuir-Nernst mixed Model and the saturated adsorption capacity of the turning point was 1.046 mg/g. The thermodynamic parameters were calculated by the equilibrium adsorption isotherm, such as standard affinity, enthalpy change and entropy change, which indicated that the adsorption of disperse dye on the pretreated PBO fiber was an exothermic process. Based on the thermodynamic and kinetic data, the adsorption of the dye on the pretreated PBO fiber was a kinetics controlled process, and the disperse dye could only diffuse into the surface layer of pretreated PBO fiber. Meanwhile, the adsorption kinetics of disperse dye on pretreated PBO fiber well agreed with a pseudo-first-order kinetic model.

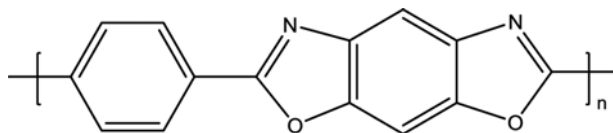Key words: PBO Fiber, Adsorption, Diffusion, Thermodynamics, Kinetics, Disperse Dye

INTRODUCTION

Poly(p-phenylene benzobisoxazole) (PBO) fiber is known to possess the highest modulus and tensile strength among all commercial manmade polymer fibers. It can be used as a reinforcing fiber in advanced composites and has great potential applications in aerospace, military and general industries [1-3]. The excellent mechanical properties, good thermal and chemical stability come from the structure character of PBO fiber with rigid chain in the chemical unit, high level of crystallinity and high degree of chain orientation along the fiber axis [4,5]. The chemical structure of PBO macromolecular unit is listed in Scheme 1.

PBO fiber is hydrophobic, the macromolecular chains of which are arranged densely and do not contain any active groups that can combine with conventional dye molecules [6,7]. This makes the dyeing and printing of PBO fiber very difficult, which limits applications of PBO fiber in some special areas such as the military camouflage. Similar to the dyeing property, compatibility problems of PBO with other polymers has puzzled both academia and industry. Therefore, since the invention of PBO fiber, many researchers worldwide

Scheme 1. Structure unit of poly(p-phenylene benzobisoxazole).

†To whom correspondence should be addressed.
E-mail: zhupxscu@163.com

continuously have worked hard in the field of PBO surface modification, based on the needs of applications of PBO fiber in fiber reinforced materials. Wu and his co-workers applied a surface modification technique to the PBO fiber with methanesulfonic acid solution to prepare reinforcement composite with epoxy resin as a matrix. They found the bonding force between fiber and epoxy resin [8]. Thereafter, Wu and Cheng utilized oxygen, nitrogen, argon or ammonia gas plasmas to modify the PBO fiber, thus introducing some polar groups, such as hydroxyl and amino groups, onto the fiber surface [9]. In addition, the roughness of modified fiber was also improved due to plasma etching and oxidation, which resulted in a significantly decreased interfacial free energy and a slightly reduced tensile strength of modified fibers [9,10]. In Liu's work, the PBO fiber was modified in a coupling agent/toluene solution with low-temperature plasma of argon. As a consequence, the contact angle of the fiber-water decreased and the shear strength between the fiber and epoxy resin increased [11]. Andreopoulos and Tarantili found that amine, amide, carbonyl, hydroxyl groups, and the like, could be added to the surface of PBO fiber by corona discharge method, which improved the wetting property along with the chemical reactivity of the fiber surface [12]. According to another report, the PBO fiber was pretreated in a solution of epichlorohydrin/acetone, and then modified by γ-ray radiation method. In this way, the modified fiber could interact well with the chemical active sites of epoxy matrixes due to some new groups containing oxygen, nitrogen and/or chlorine on the modified surface [13].

In our previous research, the polyphosphoric acid (PPA) was employed to pretreat the PBO fiber so that the micropores and axial micro streaks formed on the surface of fiber. Then the pretreated PBO fiber was dyed with disperse dyes using conventional high tem-

perature and high pressure method. The color depth, color fastness, tensile strength and flame-retardant property of the pretreated PBO fiber satisfied the requirements of military camouflage and some special industries. Meanwhile, the results, in the study of the supramolecular structure and the cross-section of pretreated and dyed samples, indicated that the etching of PPA could only occur on the fiber surface, and the basic structure of the fiber was not damaged [14].

To better understand the dyeing mechanism, we analyzed the subtle differences between disperse dyeing process of pretreated PBO fiber and that of polyester by learning the research method of polyester dyeing [15-17]. In the present study, we studied the adsorption and diffusion properties of a disperse dye in the pretreated PBO fiber in terms of the equilibrium adsorption isotherm, thermodynamic parameters (standard affinity, enthalpy change and entropy change), diffusion ability parameters (diffusion coefficient and activation energy of diffusion) and the adsorption rate equation in this paper to better understand the dyeing mechanism. Furthermore, N_2 adsorption-desorption porosimetry method first was used to evaluate and calculate the effective volume of dyestuff on dry fiber.

EXPERIMENTAL

1. Materials

Poly(p-phenylene benzobisoxazole) fiber, free of any fluorescent brightener, was supplied by Chenguang Chemical Industry Institute, Chengdu, China. To remove the oil and chemicals that clung on the fiber, it was scoured with acetone and ethanol at room temperature for 20 min respectively, washed repeatedly with hot and cold deionized water and dried under laboratory conditions. Then the PBO fiber was pretreated with polyphosphoric acid (PPA) at 65 °C for 2 min. The sample was rinsed with flowing water for 10 minutes, and was dipped in 10 g/L sodium carbonate aqueous solution for neutralization. Finally, the fiber bundles were rinsed repeatedly with hot and cold deionized water and dried under laboratory conditions. After pre-treatment process according to the above, the glass transition temperature (T_g) of the fiber was changed from 194 °C to 183 °C; the crystallinity of the sample was changed from 93.78% to 82.33% [14].

C. I. Disperse Red 60 (Scheme 2) was obtained from Dyestar Ltd. (Shanghai, China), which was used after removing dispersing agents with acetone and purifying by recrystallization. Polyphosphoric acid (PPA), acetic acid, sodium carbonate, ethanol, acetone, and N,N-dimethyl formamide were of analytical grade.

2. Measurement of Effective Volume

The samples were tested for their porosity characteristics by N_2 adsorption-desorption porosimetry at 77 K, by using a Micromerit-

Scheme 2. Chemical Formula of C. I. Disperse Red 60.

ics Tristar 3000 Surface Area and Pore Size Analyzer (US Micromeritics Ltd.). All samples were degassed for 24 h at 573 K in vacuum circumstance to remove any moisture or adsorbed contaminants that may have been present on the surface [18]. BET surface areas (S_{BET}) of the original and pretreated fibers can be measured by applying the included software based on the BET equation and the adsorption data [19]. The total pore volume was evaluated by addition of microporous and macroporous volumes [20]. The effective volume (V) of dyestuff on dry untreated and pretreated PBO fibers in adsorption process was tested by this method, the values of which are 0.036 L/kg and 0.53 L/kg, respectively.

3. Standard Curves of Absorbance-concentration of Dye Solution

Based on the Lambert-Beer Law, the concentration (g/L) of the dyebath was tested on Shimadzu UV-2401PC UV/Visible spectrophotometer under the maximal adsorption peak (λ_{max}=520 nm) of the dye. The testing solution was composed of H_2O and N,N-dimethyl formamide, of which the volume ratio of these two constituents was 1 : 1, and the pH value of the mixed solution was adjusted to 6.0± 0.2 with dilute acetic acid solution [21].

4. Equilibrium Adsorption Isotherm

The dye was dispersed in deionized water to the required concentration (0.05-1.0 g/L). The pH of the dye solution was adjusted to 6.0±0.2 with glacial acetic acid. The three kinds of fiber (0.1 g), original or pretreated PBO fiber and commercial PET fiber which were selected for comparison with the adsorption of disperse dye on normal synthetic fiber, was individually put into an Erlenmeyer flask installed with a reflux condensator and a thermostatic bath, followed by addition of the dye solution 200 mL. The ratio of the dye solution to fiber (liquor ratio) was 2,000 : 1, which could be considered as an infinite ratio. The dyeing flask was shaken for 96 hours at temperatures of 50, 70 and 90 °C, respectively. At the end of experiment, 1.0 mL of the dye residual solution was pipetted out from the experiment solution and its concentration was determined [22].

5. Standard Affinity, Enthalpy Change and Entropy Change

The standard affinity $-\Delta\mu^0$ (kJ/mol) of the dye on fibers was calculated using Eq. (1) [23,24]

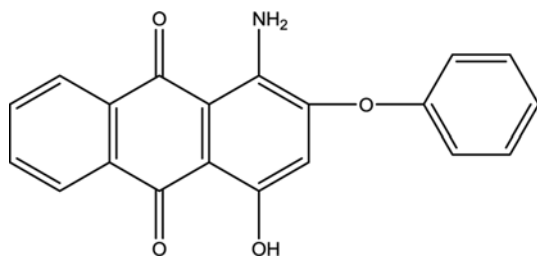$$-\Delta\mu^0 = -(\mu_f^0 - \mu_s^0) = RT\ln\frac{[D]_f}{V[D]_s} \tag{1}$$

where $-\mu_f^0$ is standard chemical potential of dye on the fiber; $-\mu_s^0$ is standard chemical potential of dye in dyeing solution; R is universal gas constant (8.314 J/mol·K); T is absolute temperature (K); $[D]_f$ is dye concentration on the fiber (mg/g); $[D]_s$ is dye concentration of the adsorption solution (mg/L); V is effective volume of dyestuff on dry fiber in adsorption process ($V_{Polyester}$=1.0 L/kg) [25].

The enthalpy change (ΔH^0) manifested as heat of adsorption (kJ/mol) in the adsorption process, which was calculated by Gibbs-Helmholtz equation Eq. (2) [23]

$$\Delta H^0 = \frac{T_2\Delta\mu_1^0 - T_1\Delta\mu_2^0}{T_2 - T_1} \tag{2}$$

where $-\Delta\mu_1^0$ and $-\Delta\mu_2^0$ are the standard affinity at different temperatures respectively; T is absolute temperature (K).

The entropy change (ΔS^0) of adsorption at different temperature (J/mol·K) was calculated using Eq. (3) [23,26]

$$-\Delta\mu^0 = T\Delta S^0 - \Delta H^0 \tag{3}$$

6. Dyeing Dynamics

The dry fiber sample of 0.1 g and 200 mL dye solution (0.02 g/L) were put in a flask with a reflux condensator, which was shaken in a temperature controlled bath under the temperatures of 50 and 90 °C, respectively. Every other period of time, 1.0 mL of dye solution was pipetted from the experiment solution to determine its concentration, so as to establish a relationship of the dye uptake and time [22].

7. Diffusion Coefficient and Activation Energy of Diffusion

According to Hill equation, Eq. (4) [27,28], the diffusion coefficient was calculated using Eq. (5) [28].

$$\frac{C_t}{C_\infty} = 4\left(\frac{D_f \cdot t}{\pi \cdot r^2}\right)^{1/2} \tag{4}$$

where C_t is dye exhaustion at time t (mg/g); C_∞, dye exhaustion at equilibrium (mg/g); D_f, diffusion coefficient (m^2/min); r, radius of fiber (μm) which was measured by scanning electron microscope (Hitachi, Ltd., Tokyo, Japan), and the radii of polyester and PBO fiber are 4.48 and 10.95 μm, respectively [14]. When (C_t/C_∞)=0.5, t=$t_{1/2}$, Eq. (4) was changed to

$$D_f = \frac{0.06292 r^2}{t_{1/2}} \tag{5}$$

According to the Arrhenius equation, Eq. (6) [14], the activation energy of the diffusion was calculated from the relationship between lnD and 1/T

$$\ln\frac{D_1}{D_2} = \frac{E}{R}\left(\frac{1}{T_2} - \frac{1}{T_1}\right) \tag{6}$$

where D_1 and D_2 are diffusion coefficients at different temperatures, respectively (m^2/min); E is activation energy (kJ/mol);. T_1 and T_2 are different experimental temperature, respectively.

8. Adsorption Rate Equation

Pseudo-first-order equation, also known as the Lagergren equation, is expressed as follows [22,29-31]:

$$\frac{dC_t}{dt} = k_1(C_\infty - C_t) \tag{7}$$

where k_1 is the rate constant for pseudo first-order adsorption (min^{-1}). Integrating Eq. (7) and applying initial conditions, the Eq. (7) was changed to

$$\log(C_\infty - C_t) = \log C_\infty - \frac{k_1}{2.303}t \tag{8}$$

and

$$h_{i,1} = k_1 C_\infty \tag{9}$$

where $h_{i,1}$ (mg/g·min) is the initial dye adsorption rate of pseudo-first-order adsorption.

The pseudo-second-order kinetic model is based on adsorption equilibrium capacity and can be expressed as follows [22,29-31]:

$$\frac{dC_t}{dt} = k_2(C_\infty - C_t)^2 \tag{10}$$

where k_2 is the rate constant for pseudo second-order adsorption

(g/mg·min). By integrating Eq. (10) and applying the initial conditions, it gives:

$$\frac{t}{C_t} = \frac{1}{k_2 C_\infty^2} + \frac{t}{C_\infty} \tag{11}$$

and

$$h_{i,2} = k_2 C_\infty^2 \tag{12}$$

where $h_{i,2}$ (mg/g·min) is the initial dye adsorption rate of pseudo-second-order adsorption.

RESULTS AND DISCUSSION

1. Equilibrium Adsorption Isotherm

The equilibrium adsorption isotherm, which was plotted with adsorbate concentration on adsorbent as ordinate against adsorbate concentration in solution as abscissa, was fundamental in describing the interaction behavior between adsorbate and adsorbent. It is important in the design of an adsorption system and a dyeing process [21,31]. Figs. 1 and 2, respectively, show the isotherms of the adsorption of disperse dye on polyester and original PBO fiber at 50, 70 and 90 °C. The scattered points in Fig. 1 indicate a linear increasing in the disperse dye concentration on the polyester fiber ([D]$_f$) with increasing of the disperse dye concentration in solution ([D]$_s$) at different experimental temperatures. That is, the ratio of [D]$_f$ and [D]$_s$ was a constant. These three adsorption isotherms were fitted with Eq. (13) by lines in Fig. 1, and the adsorption model was generally named the Nernst model. So the adsorption process of the disperse dye on the polyester can be regarded as a distribution between two immiscible solvents (water and fiber). The isotherm parameters of disperse dye on polyester are listed in Table 1. This result was consistent with previously published literature [15].

$$[D]_f = [D]_N = K_N [D]_s \tag{13}$$

where [D]$_N$ is the disperse dye concentration on polyester fiber calculated based on the Nernst adsorption model (mg/g); K_N is the partition coefficient of the Nernst adsorption model (L/g).

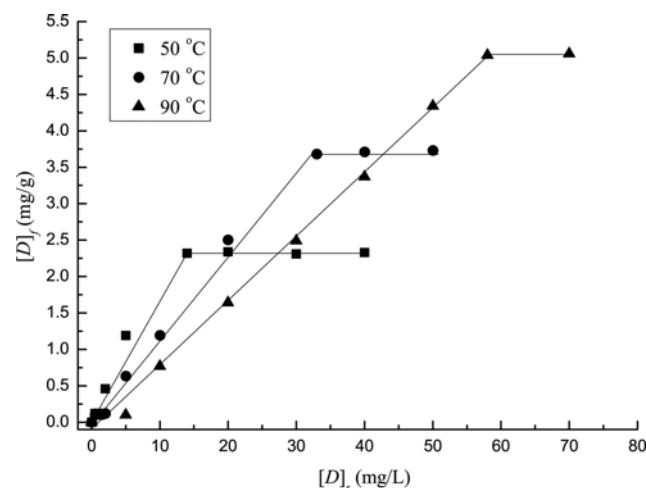In Fig. 2, although the dye concentration on the unpretreated PBO
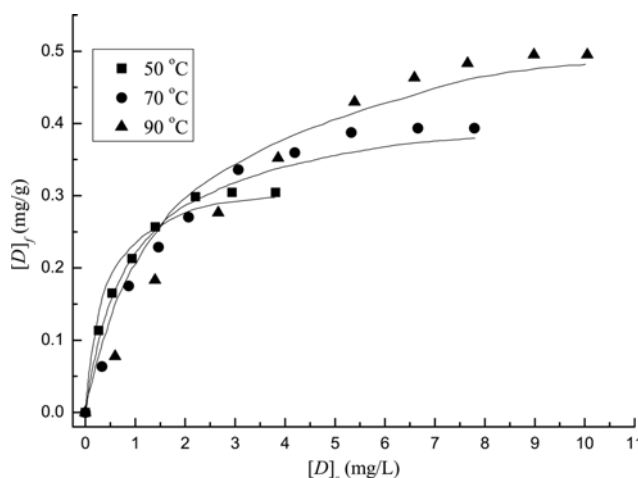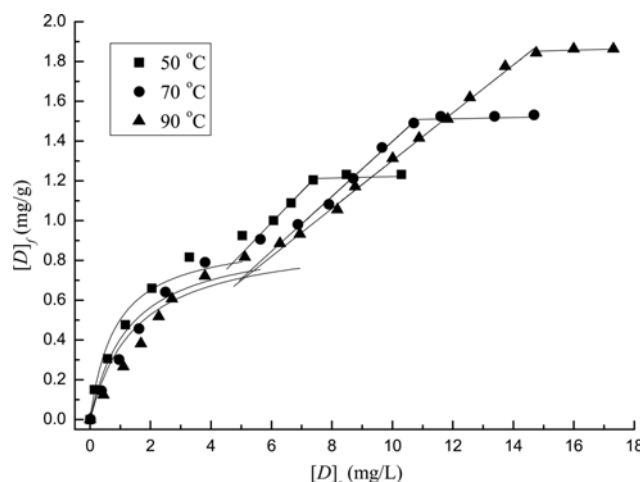

Fig. 1. Adsorption isotherms of the disperse dye on polyester fiber at 50, 70 and 90 °C.

Table 1. Adsorption isotherm parameter of disperse dye on polyester and original PBO fibers

Temperature	Polyester			Original PBO		
	K_N (L/g)	$[S]_P$ (mg/g)	R^2	K_L (L/g)	$[S]_o$ (mg/g)	R^2
50 °C	0.167	2.332	0.96616	2.935	0.306	0.97125
70 °C	0.115	3.731	0.99291	1.214	0.394	0.95364
90 °C	0.088	5.066	0.99681	0.707	0.495	0.92395

$[S]_P$ and $[S]_o$ the max equilibrium adsorption capacity of the disperse dye on polyester and original PBO fibers, respectively; K_N partition coefficient of the *Nernst* model; K_L equilibrium adsorption constant of the *Langmuir* model; R^2 correlation coefficient

Fig. 2. Adsorption isotherms of the disperse dye on original PBO fiber at 50, 70 and 90 °C.

Fig. 3. Adsorption isotherms of the disperse dye on pretreated PBO fiber at 50, 70 and 90 °C.

fiber ($[D]_f$) also increased with increasing $[D]_s$ the rising trend gradually slowed down in a higher concentration range of $[D]_s$. The three sets of scattered data points were fitted with Eq. (14) by Origin 8.0, a common drawing and analysis software. All the three fitted curves accorded with the Langmuir adsorption model. The phenomenon indicated that the adsorption of the disperse dye on the untreated PBO fiber basically belonged to a monolayer adsorption which might be based on the aromatic and benzobisoxazole ring as the adsorption centers. The detailed isotherm parameters are also listed in Table 1.

$$[D]_f = [D]_L = \frac{K_L[D]_s[S]}{1+K_L[D]_s} \qquad (14)$$

where $[D]_L$ is the disperse dye concentration on the untreated PBO fiber calculated based on the Langmuir adsorption model (mg/g); $[S]$ is the max equilibrium adsorption capacity of the disperse dye on PBO fiber (mg/g); K_L is the equilibrium adsorption constant of the Langmuir model (L/g).

Meanwhile, by comparison of the isotherm parameters in Table 1, the max equilibrium adsorption capacity ($[S]$) of disperse dye on both the polyester and untreated PBO fibers increased with rising experimental temperature, while the max equilibrium adsorption capacity of polyester ($[S]_P$) was larger than that of untreated PBO ($[S]_o$) at every temperature in the experiment. A reasonable explanation was that, on one hand, the higher temperature promoted swelling of fibers and thermal motion of disperse dye molecules, and the dye molecule could overcome an energy barrier to diffuse into the polyester fiber. On the other hand, under existing temperature

condition, the disperse dye molecules almost could not diffuse into the interior of the PBO fiber because of much higher crystallinity and orientation degree of the PBO fiber than ordinary fibers, e.g., the polyester fiber. For the same reason, the dye molecules could only adsorb on the PBO fiber surface, so the rising trend of $[S]_o$ with temperature was lower than that of $[S]_P$. This inference was confirmed in analyzing the cross-section of dyed PBO fiber in our previous research [14]. Furthermore, the phenomenon that the correlation coefficient (R^2) values in PBO adsorption experiment became smaller with rise in the temperature indicated the diffusion ability of dye molecules to the core of PBO fiber was enhanced at higher temperature; so the adsorption isotherm gradually deviated from the Langmuir model, and was close to the Nernst model. Conversely, the value of R^2 in polyester adsorption experiment was increased.

Fig. 3 shows the adsorption isotherms of the disperse dye on the PBO fiber pretreated with PPA at 50, 70 and 90 °C, respectively. In the figure, the $[D]_f$ increased with increasing the $[D]_s$ as a whole at every temperature. But the figure details suggested two plateau regions on the curves of relationship between $[D]_f$ and $[D]_s$ at different temperatures. The surprising phenomenon became clearer as some guide lines were fitted in Fig. 3 based on experimental data, by Langmuir adsorption model (Eq. (13)) and Nernst adsorption model (Eq. (14)), respectively. When the $[D]_s$ is lower than a certain value between 4-6 mg/L, the increasing of $[D]_f$ with $[D]_s$ represented a character of Langmuir adsorption mode. That is, dye molecules tended to come into being monolayer adsorption on the fiber surface. Contrarily, when the $[D]_s$ was higher than this fixed value, the changes of $[D]_f$

with $[D]_s$ turned to perform a Nernst adsorption model. Therefore, the dyeing process of the pretreated PBO fiber with the disperse dye underwent a mixed Langmuir-Nernst adsorption model. At dyeing temperatures far below the T_g of PBO in the experiment, dye molecules still could not easily enter into matrix of the pretreated fiber [14]. Therefore, in the low dye concentration, dye molecules tended to come into being monolayer adsorbing at micropore and striation situation on the fiber surface owing to the interaction between dye molecules and benzene and benzobisoxazole ring. Only when the concentration of dye was sufficiently higher did the dye molecules in the solution gradually diffuse into the pretreated fiber, which was driven by a large enough concentration gradient between outside and interior of fiber.

Furthermore, the max equilibrium adsorption capacity at the Nernst part ($[S]_N$) on the pretreated PBO fiber became larger at the higher temperature, which is similar to the phenomenon in the polyester experiment. The result presented another driven force of the Nernst adsorption model. At a higher temperature, dye molecules had more energy to move to the porous subsurface of the pretreated PBO fiber. However, the max equilibrium adsorption capacity at the Langmuir part $[S]_L$ was almost constant at the three experimental temperatures.

On one hand, the micropore and striation on the pretreated PBO fiber surface was large enough for the disperse dye molecules adsorption. So, at higher than 50 °C, dye molecules monolayer adsorption could occur at these positions. On the other hand, below the T_g, because PBO macromolecular chain segments could not move, and the attraction between the dye molecules and the PBO macromolecules was greater than the thermal motion energy of the dye molecules diffusing into the fiber, the dye molecules apparently more tended to adsorb on the fiber surface. So the $[S]_L$ was nearly no change, when the temperature rose from 50 °C to 90 °C. Meanwhile, by comparing the values of R^2 of the three fitted curves in Table 2, the value decreased in the Langmuir stage and then increased in the Nernst stage as the experimental temperature rose. The results showed the transition of the Langmuir adsorption to the Nernst adsorption mode.

To further determine the isothermal equation and the adsorption isotherm turning point ($[S]_L$) of disperse dye adsorption on the pretreated PBO fiber, the experimental data in Fig. 3 was used and the relationship between $1/[D]_F$ and $1/[D]_s$ was plotted as shown in Fig. 4. The linear relationship also further indicated a Langmuir model adsorption when $[D]_F<[S]_L$ in the adsorption of disperse dye on the pretreated PBO fiber. Then the three lines were extended and the coordinate values of the three intersections were (0.059, 0.852), (0.157, 1.078) and (0.116, 0.940), respectively. The average of coordinate values of the three points was (0.111, 0.956), well consistent with
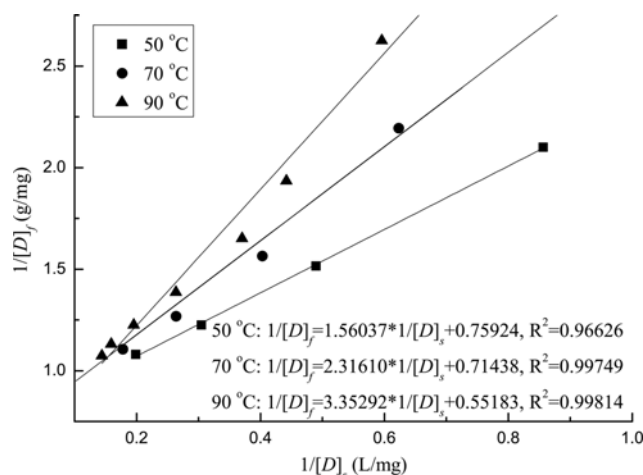

Fig. 4. Relationship between reciprocal of $[D]_f$ and $[D]_s$.

the averaged reciprocal of the coordinate value (9.040, 1.046) of the three turning points in Fig. 3 for the adsorption isotherms. From this ordinate $[S]_L$ can be obtained. That is, the max equilibrium adsorption capacity of the disperse dye on the pretreated PBO at Langmuir part was equal to 1.046 mg/g. At all $[D]_s$, the equilibrium adsorption of disperse dye on pretreated PBO fiber, $[D]_f$, could be calculated by:

$$[D]_f=[D]_L=\frac{K_L[D]_s[S]_L}{1+K_L[D]_s}, \text{ when } [D]_s<9.040 \text{ mg/L} \tag{15}$$

$$[D]_f=[D]_N=K_N[D]_s, \text{ when } [D]_s>9.040 \text{ mg/L} \tag{16}$$

and

$$[D]_f=[S]_L=1.046, \text{ when } [D]_s=9.040 \text{ mg/L} \tag{17}$$

where $[D]_L$ and $[D]_N$ are the disperse dye concentrations on pretreated PBO fiber at the Langmuir part and Nernst part of equilibrium adsorption isotherm, respectively (mg/g); $[S]_L$ is the disperse dye saturated adsorption capacity on pretreated PBO fiber at the Langmuir part (mg/g); K_N is the partition coefficient of the Nernst model adsorption (L/g); K_L is the equilibrium adsorption constant of the Langmuir model adsorption (L/g). The adsorption isotherm parameters of the disperse dye on the pretreated PBO fiber at 50, 70 and 90 °C are shown in Table 2.

Moreover, the partition coefficient of the Nernst model adsorption (K_N) and the equilibrium adsorption constant of the Langmuir model adsorption (K_L), in Table 2, are used to represent the adsorp-

Table 2. Adsorption isotherm parameter of disperse dye on pretreated PBO fiber

Temperature	Langmuir adsorption			Nernst adsorption		
	K_L (L/g)	$[S]_L$ (mg/g)	R^2	K_N (L/g)	$[S]_N$ (mg/g)	R^2
50 °C	1.184	0.925	0.95346	0.155	1.231	0.98968
70 °C	0.779	0.905	0.92683	0.138	1.531	0.99016
90 °C	0.661	0.932	0.89663	0.120	1.864	0.99360

$[D]_L$ and $[D]_N$ the disperse dye concentrations on pretreated PBO fiber at the *Langmuir* part and *Nernst* part of equilibrium adsorption isotherm, respectively; $[S]_L$ and $[S]_N$ the saturated adsorption capacity of the disperse dye on pretreated PBO fiber at the *Langmuir* part and *Nernst* part; K_N partition coefficient of the *Nernst* model; K_L equilibrium adsorption constant of the *Langmuir* model; R^2 correlation coefficient

tion degree of the adsorbate in the adsorbent at Nernst and Langmuir adsorption processes, respectively. A greater value denotes a greater significant adsorption tendency in the same adsorption process. In the three sets of experiment data, both the K_N and the K_L decreased with increase of the temperature, no matter what fiber, polyester, original PBO or pretreated PBO fiber, was involved in the adsorption of the disperse dye. This result indicated that the elevated temperature was not conducive for adsorption because the adsorption process was an exothermic process. The specific reasons will be discussed in detail in the following section.

2. The Standard Affinity, the Enthalpy Change and the Entropy Change

The standard affinity, enthalpy change and entropy change are usually employed to describe the dyeing ability of a given dyestuff on a fiber, which were obtained according to thermodynamic theory. In a specific dyeing system, these values depend on the properties of the dye and fiber involved when the temperature, pressure and the amount of other components remain constant [28,32]. Because the adsorption isotherm types of the disperse dye on the untreated and the pretreated PBO fiber were Langmuir model and Langmuir-Nernst mixed model, respectively, the thermodynamic parameters of the former adsorption and the front part of the latter adsorption would change with the alteration of the values of $[D]_f$ and $[D]_s$. So these parameters of the relevant adsorption isotherms were not listed. The adsorption isotherms of the disperse dye on the polyester and the pretreated PBO fiber after $[D]_f>[S]_L$ could be expressed by Nernst model, so the standard affinity, the enthalpy change and the entropy change of disperse dye on both fibers could be calculated using Eq. (1)-(3) and the data are shown in Table 3.

The standard affinity is a measure of the tendency of the dye moving from its standard state in solution to its standard state in fiber. The larger the value of standard affinity is, the larger the adsorption tendency of a dye on fiber [28]. In Table 3, the standard affinity values of the dye on the polyester were similar with that on the pretreated PBO at 50 °C and 90 °C, respectively. This result showed that the disperse dye could adsorb on the pretreated PBO fiber as well as on the polyester, and proved that dyeing the pretreated PBO fiber with disperse dye was practicable. Meanwhile, the changes of the enthalpy values for these two adsorption processes were less than zero. This phenomenon demonstrated that the disperse dyeing processes of both the polyester and pretreated PBO were exothermic, and the higher temperature for the adsorption of the dye on the fiber was disadvantageous and polyester fiber was more unfavorable. The change of standard affinity declined with increase of temperature for the two kinds of fibers, also directly confirming this result.

Entropy in thermodynamics is a measure of the unavailability of a system's energy to do work, and has often been loosely associated with the degree of order, disorder, and/or chaos in a thermodynamic system [28,33]. Based on the parameters in Table 3, both the values of entropy change for the two fibers were negative, but the value of polyester was lower. In an adsorption process, the thermal motion of dye molecules was limited because of the interaction between dye molecular and fiber, and the degree of chaos in this thermodynamic system was decreased. Because the heat release and the entropy reduction of dyeing polyester were greater than that of pretreated PBO, the disperse dye adsorption on pretreated PBO was easier than on the polyester only from the viewpoint of thermodynamics. But the experimental result was just the opposite. As we know the dyeing capacity is mainly determined by the amount of amorphous part of fiber except surface area of the fiber. The actually bad dyeing performance must be that the glass transition temperature of PBO was far higher than that of polyester, so the dye molecules diffusion in the pretreated PBO fiber was more difficult than in the polyester at the experimental temperature. Therefore, the impact of kinetic factors on the dyeing process is more important than that of thermodynamic factors. In other words, the disperse dyeing of the pretreated PBO fiber was a kinetic controlled process.

3. The Diffusion Coefficient and the Activation Energy

It is generally agreed that the dyeing process involves three continuous steps [28]. The first step is usually the movement of dye in solution through the aqueous medium onto the fiber. The second step is the adsorption of dye on the surface of fiber. Then the adsorbed dye molecules diffuse into the fiber core from the fiber surface. The second step, the actual adsorption process, is generally assumed to be much more rapid than the other steps. Of the other two steps, the diffusion of the dye into the inner layer is much slower than the movement of dye through the aqueous solution due to the physical obstruction of the network of fiber molecules for dye diffusion [28].

The adsorption kinetic curves of Disperse Red 60 on polyester, untreated PBO and pretreated PBO fiber are, respectively, described in Fig. 5. These curves show that a higher dyeing temperature would result in a higher adsorption rate at initial dyeing stage for all adsorption processes. By comparing the shape of each curve, the change of polyester curves at different temperatures is the most obvious
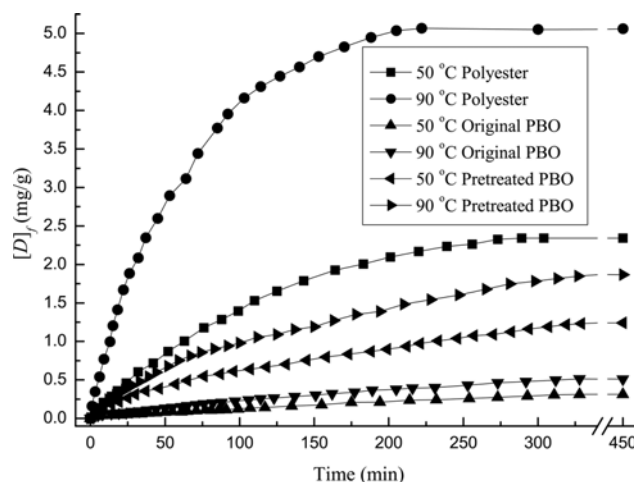
Table 3. The standard affinity, enthalpy change and entropy change of the disperse dye on the polyester and pretreated PBO fibers

Sample	$-\Delta\mu^0$ (kJ/mol)		$-\Delta H^0$ (kJ/mol)	$-\Delta S^0$ (J/mol·K)
	50 °C	90 °C		
Polyester	13.75	12.03	27.64	43.00
Pretreated PBO	13.55	12.86	19.12	17.24

Fig. 5. Adsorption rate of the disperse dye on different fibers at 50 and 90 °C.

Table 4. The diffusion coefficient and the activation energy of the disperse dye on three kinds of fibers

Fiber	$D_f (\times 10^{-14} \, m^2/min)$		E (kJ/mol)
	50 °C	90 °C	
Polyester	1.468	3.007	17.47
Original PBO[a]	0.921	1.059	3.40
Pretreated PBO[a]	1.207	1.372	3.12

D_f diffusion coefficient; E diffusion activation energy

[a]The dyed layer thickness of PBO fibers was approximately 2/5 radius of fiber, determined the dyed fiber cross sections under light microscopy, and so r=2/5×10.95 μm was used to calculate the D_f of untreated and pretreated PBO [28]

and the effect of temperature, from 50 °C to 90 °C, on the original PBO almost could be ignored. With the increasing of dyeing temperature, especially at 90 °C, which is higher than the glass transition temperature of polyester, the thermal motion of polyester macromolecular chain was intensified and the diffusion energy of the dye molecules was increased simultaneously. So the slope of adsorption kinetic curve and equilibrium adsorption capacity increased markedly. On the contrary, because the glass transition temperature of the original PBO is far higher than all the dyeing temperature, less effect of temperature on the thermal motion of PBO macromolecules was observed at 90 °C and the curve of untreated PBO was almost no change. These phenomena also further indicated that the adsorption of disperse dye on the pretreated PBO fiber was a kinetically controlled process.

Diffusion coefficient and activation energy are commonly used to express the diffusion ability of dye molecule within the fiber. The higher diffusion coefficient or lower activation energy indicate a smaller resistance for diffusion of the dye molecule within the fiber [33]. The data in Table 4 suggests that, for every fiber experimented, the diffusion coefficient of Disperse Red 60 was, respectively, increased with the temperature raised, but the ascending trend of polyester was the most obvious. This detailed reason is similar to that of the change of adsorption kinetic curve discussed in the former paragraph. Meanwhile, at the same temperature, the diffusion coefficient of polyester fiber was the largest while that of the original PBO fiber was the smallest. Because the original and pretreated PBO fibers have higher crystallinity and higher glass transition temperatures than the polyester [14], the diffusion of dye molecules into PBO fibers was more difficult. At a higher temperature in the experiment, especially 90 °C that is higher than T_g of the polyester but much lower than that of the PBO fibers, it was more beneficial to disperse dye to diffuse into the polyester fiber.

A seemingly abnormal phenomenon was observed as for the diffusion activation energy in comparison with the actual dyeing process. The values of the untreated and pretreated PBO fibers were smaller than that of the polyester, which seemed to indicate that the dye diffusion was easier for dyeing PBO fibers. A possible reason was that the disperse dye only diffused into the surface layer of PBO and almost could not penetrate into the core of fiber although the PBO fiber was swelled and etched by polyphosphoric acid [14]. So the radius value of the pretreated PBO fiber in Eq. (5) was two-fifths of the actual radius of the fiber which was used to calculate

the diffusion coefficient of PBO [28]. In fact, in the dyeing process of the pretreated PBO fiber the dynamic activation energy was more relative to the adsorption at fiber surface or absorption in the subsurface, which must be lower than the diffusion activation energy into the fiber matrix in dyeing the polyester.

4. The Adsorption Rate Equation

To further study the adsorption dynamics of disperse dye on the pretreated PBO fiber, pseudo-first-order and pseudo-second-order equations were used to test the experimental data in Fig. 5. Based on Eqs. (8) and (11), adsorption rate curves were drawn as $\log(C_\infty - C_t)$ and t/C_∞ against time for the adsorption of disperse dye on pretreated PBO fiber, and shown in Figs. 6 and 7, respectively. The dye exhaustion at equilibrium (C_∞) and the rate constants (k_1 and k_2) could be calculated by the slopes and intercepts of the two lines in Figs. 6 and 7 respectively, and the initial adsorption rate of two kinds of dynamic models ($h_{i,1}$ and $h_{i,2}$) are given in Table 5. In the table, the correlation coefficient (R^2) of pseudo-first-order equation was higher than that of pseudo-second-order equation at different temperatures. This result shows that this adsorption process might more accord
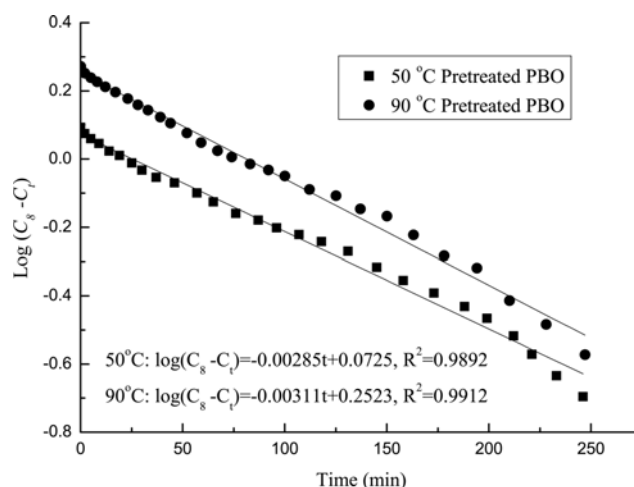

50 °C: $\log(C_\infty - C_t) = -0.00285t + 0.0725$, $R^2 = 0.9892$

90 °C: $\log(C_\infty - C_t) = -0.00311t + 0.2523$, $R^2 = 0.9912$

Fig. 6. The plot of pseudo first-order equation for adsorption of the disperse dye on pretreated PBO fiber at 50 and 90 °C.

50 °C: $t/C = 0.61756t + 83.5093$, $R^2 = 0.94296$

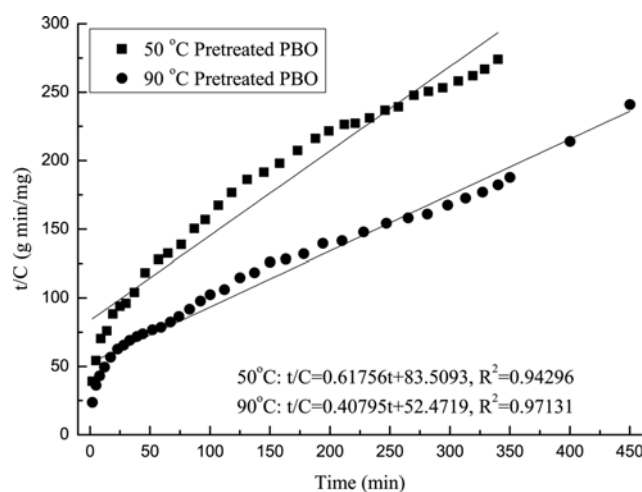90 °C: $t/C = 0.40795t + 52.4719$, $R^2 = 0.97131$

Fig. 7. The plot of pseudo second-order equation for adsorption of the disperse dye on pretreated PBO fiber at 50 and 90 °C.

Table 5. The rate parameters of disperse dye on pretreated PBO fiber

Temperature (°C)	C_∞ (mg/g)	Pseudo first-order adsorption			Pseudo second-order adsorption		
		k_1 (min^{-1})	$h_{i,1}$ (mg/g·min)	R^2	k_2 (g/mg·min)	$h_{i,2}$ (mg/g·min)	R^2
50	1.20	7.05×10^{-3}	8.74×10^{-3}	0.9892	1.01×10^{-2}	1.55×10^{-2}	0.94296
90	1.81	4.86×10^{-2}	9.04×10^{-3}	0.9912	7.32×10^{-2}	2.53×10^{-2}	0.97131

k_1 the rate constant for pseudo first-order adsorption (min^{-1}); k_2 the rate constant for pseudo second-order adsorption (g/mg·min); $h_{i,1}$ the initial adsorption rate of pseudo first-order (mg/g·min); $h_{i,2}$ the initial adsorption rate of pseudo second-order (mg/g·min); R^2 correlation coefficient

with the pseudo-first-order model than the pseudo-second-order equation. The C_∞ values obtained also basically agreed with the experimental data ($C_{\infty,50}$=1.24 mg/g, $C_{\infty,90}$=1.86 mg/g). Moreover, by comparing the rate constant (k_1) and the initial adsorption rate ($h_{i,1}$) at different temperatures, both the k_1 and $h_{i,1}$ values at higher temperature were higher. The phenomenon indicated that a higher temperature was beneficial to disperse dyeing of synthetic fibers.

CONCLUSIONS

Dyeing properties of C. I. disperse Red 60 in PBO fiber pretreated with polyphosphoric acid were investigated. At the same time the adsorption thermodynamic and kinetic characteristics of the disperse dye on the pretreated PBO fiber were compared with that on the polyester fiber and original PBO fiber. The adsorption isotherm of disperse dye on pretreated PBO fiber was a mixed Langmuir-Nernst model. As the temperature increased, the adsorption isotherm gradually shifted to the Nernst model. And the adsorption isotherm parameters of the disperse dye on the pretreated PBO fiber were calculated, and the saturated adsorption capacity of the disperse dye on the pretreated sample at the Langmuir part of adsorption isotherm was 1.046 mg/g. The data of the standard affinity, the enthalpy change and the entropy change of adsorption of the disperse dye on the pretreated PBO fiber demonstrated that the adsorption of disperse dye onto the pretreated PBO fiber was an exothermic process. It also proved that this dyeing process was a kinetic controlled process.

By comparing the diffusion coefficient and the activation energy of disperse dye on various fibers, the diffusion of the disperse dye in the pretreated PBO fiber was nearly the same as in polyester fiber, but this process actually occurred only in the surface layer of the PBO fiber. The pseudo-first or second-order kinetic models were used to verify the adsorption kinetics data. The dynamical behavior of disperse dye adsorption on the pretreated PBO fiber was more in line with pseudo-first-order kinetic model (R^2>0.99), and the values of rate constant and initial adsorption rate became large with the temperature increasing.

The results and analyses were significant for the PBO fiber with high performance and with difficulty to be dyed, although the dyeing temperature was far below the T_g of the fiber in the existing limited conditions. We are planning to further study the dyeing property at much higher temperatures, and by means of some dyeing carriers to meet the actual demands for the dyed PBO fibers.

ACKNOWLEDGEMENT

REFERENCES

1. S. Bourbigot, X. Flambard and S. Duquesne, *Polym. Int.*, **50**, 157 (2001).
2. H. G. Chae and S. Kumar, *J. Appl. Polym. Sci.*, **100**, 791 (2006).
3. T. Zhang, D. Hu, J. Jin, S. Yang, G. Li and J. Jiang, *Appl. Surf. Sci.*, **256**, 2073 (2010).
4. D. Feng, S. Wang, Q. Zhuang, P. Wu and Z. Han, *Polymer*, **45**, 8871 (2004).
5. B. Song, Q. Fu, L. Ying, X. Liu, Q. Zhuang and Z. Han, *J. Appl. Polym. Sci.*, **124**, 1050 (2012).
6. J. F. Wolfe and F. E. Arnold, *Macromolecules*, **14**, 909 (1981).
7. J. F. Wolfe, B. H. Loo and F. E. Arnold, *Macromolecules*, **14**, 915 (1981).
8. G. M. Wu, C. H. Hung, J. H. You and S. J. Liu, *J. Polym. Res.*, **11**, 31 (2004).
9. G. M. Wu and C. H. Chang, *Vacuum*, **81**, 1159 (2007).
10. P. Chen, C. Zhang, X. Zhang, B. Wang, W. Li and Q. Lei, *Appl. Surf. Sci.*, **255**, 3153 (2008).
11. D. Liu, J. Hu, Y. Zhao, X. Zhou, P. Ning and Y. Wang, *J. Appl. Polym. Sci.*, **102**, 1428 (2006).
12. A. G. Andreopoulos and P. A. Tarantili, *J. Elastom. Plast.*, **30**, 118 (1998).
13. C. H. Zhang, Y. D. Huang and Y. D. Zhao, *Mater. Chem. Phys.*, **92**, 245 (2005).
14. Y. Guan, Y.-h. Mao, Q.-m. Kong, X.-f. Zeng and P.-x. Zhu, *Color. Technol.*, n/a (2013).
15. M. J. Schuler and W. R. Remington, *Discuss. Faraday Soc.*, **16**, 201 (1954).
16. O. Glenz, W. Beckmann and W. Wulder, *J. Soc. Dyers Colour.*, **75**, 141 (1959).
17. D. Patterson and R. P. Sheldon, *T. Faraday Soc.*, **55**, 1254 (1959).
18. A. K. Ladavos, A. P. Katsoulidis, A. Iosifidis, K. S. Triantafyllidis, T. J. Pinnavaia and P. J. Pomonis, *Micropor. Mesopor. Mater.*, **151**, 126 (2012).
19. E. P. Barrett, L. G. Joyner and P. P. Halenda, *J. Am. Chem. Soc.*, **73**, 373 (1951).
20. N. Passe-Coutrin, S. Altenor, D. Cossement, C. Jean-Marius and S. Gaspard, *Micropor. Mesopor. Mater.*, **111**, 517 (2008).
21. Y.-H. Mao, Y. Guan, Q.-K. Zheng, X.-N. Feng and X.-X. Wang, *Cellulose*, **18**, 271 (2011).
22. M. S. Chiou and H. Y. Li, *Chemosphere*, **50**, 1095 (2003).
23. J. R. Aspland and C. L. Bird, *J. Soc. Dyers Colour.*, **77**, 9 (1961).
24. H. Gerber, *J. Soc. Dyers Colour.*, **110**, 375 (1994).
25. T.-K. Kim, Y.-A. Son and Y.-J. Lim, *Dyes Pigm.*, **72**, 246 (2007).

26. C. L. Bird and M. P. Harris, *J. Soc. Dyers Colour.*, **73**, 199 (1957).

27. K. H. Park, M. Casetta and V. Koncar, *Color. Technol.*, **118**, 319 (2002).

28. T. Vickerstaff, *The physical chemistry of dyeing*, London, Oliver & Boyd (1954).

29. M. Chairat, S. Rattanaphani, J. B. Bremner and V. Rattanaphani, *Dyes Pigm.*, **64**, 231 (2005).

30. M. Chairat, S. Rattanaphani, J. B. Bremner and V. Rattanaphani, *Dyes Pigm.*, **76**, 435 (2008).

31. M.-S. Chiou and H.-Y. Li, *J. Hazard. Mater.*, **93**, 233 (2002).

32. I. D. Rattee and M. M. Breuer, *The physical chemistry of dye adsorption*, London, Academic Press (1974).

33. J. Crank, *The mathematics of diffusion*, London, Oxford University Press (1975).